Final version published as: Kaake, L.G. Designs for Donor-Acceptor Copolymer Based Double Heterojunction Solar Cells. *ACS Energy Letters*. 2017. 2(7), 1677-1682. DOI: 10.1021/acsenergylett.7b00519

# Designs for Donor-Acceptor Copolymer Based Double Heterojunction Solar Cells

*Loren G. Kaake**

Simon Fraser University, Department of Chemistry, 8888 University Dr., Burnaby, BC V5A 1S6, Canada

**Corresponding Author**

*Email: lkaake@sfu.ca

**ABSTRACT**

Self-consistent field calculations were used to examine a design motif for organic double heterojunction solar cell materials. They are a specific type of cascade heterojunction designed to increase cell voltage without sacrificing current and consist of fully conjugated block polymers. The design employs three sections; a p-type section, an n-type section and a third section called the bridge. The energy alignment between sections is important to optimal device function and a motif based on electron donating and electron accepting subunits was evaluated. If the energetic offset between p-type and n-type sections is greater than the exciton binding energy and if the bridge is formed using the scheme presented, a nearly ideal energetic alignment is obtained. In addition, calculations on the excited states of the system were performed to illustrate the relationship between bridge length and the magnitude of charge carrier recombination currents. An order of magnitude decrease relative to the corresponding diblock polymer

can be expected for bridge lengths of > 6 repeat units. Taken in sum, these results offer concrete guidelines for the development of synthetic targets in this promising class of materials.

**TOC GRAPHIC**

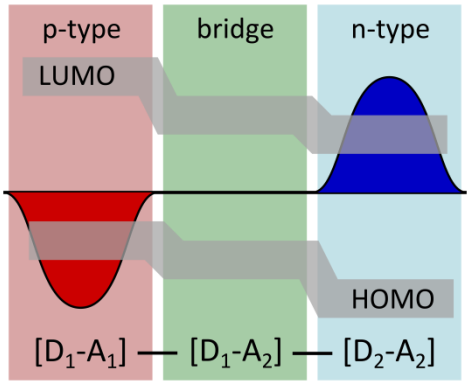


The development of solar cells with high efficiency and low cost is both an important goal for the mitigation of climate change and presents an economic opportunity.[1,2] Photovoltaic devices that use π-conjugated molecules and polymers as their active layer have improved dramatically since their early demonstrations[3-5] to become viable technologies for large-area, low-cost, flexible and building integrated photovoltaics.[6] Indeed numerous examples of lab-scale devices[7-9] have met the ambitious goal of producing cells with > 10% power conversion efficiency.[10] However, new materials including metal-halide perovskites[11] can be leveraged to make solar cells of nearly double this power conversion efficiency.[12] In addition, the rate of recent progress in organic photovoltaics seems to hint at the possibility that obstacles of a more fundamental nature are currently limiting cell efficiencies.[13,14]

In response to these challenges, researchers are exploring the possibilities of energy cascade structures/ternary blends[15-21] and singlet fission[22,23] amongst other approaches to improve devices beyond the current paradigm of two-component bulk heterojunction cells. Often, these strategies are aimed at increasing cell current by improving the external quantum efficiency of photocurrent generation. To improve the open circuit voltage ($V_{OC}$) of a cell without sacrificing cell current, we

proposed a double heterojunction based on a fully conjugated triblock polymer system and performed a series of simulations that suggested power conversion efficiencies approaching 30% were possible.[24] Achieving the full potential of these devices requires excellent phase separation and careful energetic alignment of each section of the polymer. In addition, synthetic targets were identified from the literature and the thickness dependence of their power conversion efficiency was calculated. However, a more general connection between the electronic structure of the material and its chemical constituents was only hinted at, making it difficult to design synthetic targets and risky to carry out a challenging synthesis. To address this shortcoming, we performed self-consistent field calculations on a general structural motif based on electron donating and electron accepting subunits in an attempt to aid synthetic chemists interested in these materials.

In more detail, the double heterojunction structure is a specific type of cascade heterojunction, consisting of three fully conjugated sections, a p-type section, an n-type section, and a bridge section connecting the two (see Fig. 1). The key design principle that differentiates the double heterojunction solar cell from other fully conjugated block polymer solar cell materials[25-40] is the bridge section. Specifically, the maximum efficiency for a double heterojunction solar cell is only obtained when all recombination currents flow across the bridge.[24] This factor sets stringent requirements on phase purity and differentiates it from ternary systems[20] because the electronic, not optical properties of the bridge are of primary concern. The bridge provides a synthetic handle to eliminate the standard charge transfer state pathway for recombination, increasing $V_{OC}$ by inhibiting recombination

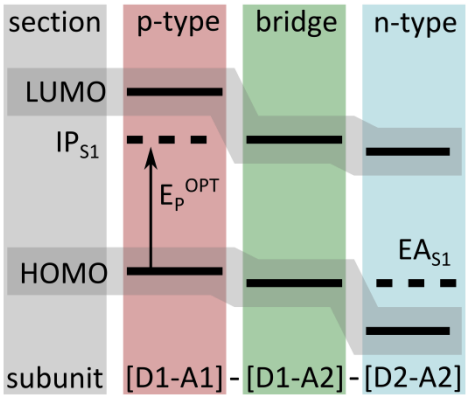


Figure 1. Schematic of an organic double heterojunction. The HOMO level refers to the ionization potential of the ground state while the LUMO refers to the electron affinity of the ground state. $IP_{S1}$ and $EA_{S1}$ refers to the ionization potential and electron affinity of the singlet exciton, respectively.

without a large energy offsets between the sections. In bulk heterojunction cells, large energy offsets decrease open circuit voltage but are necessary to prevent charge recombination by ensuring that charge transfer excitons cannot be converted into triplet excitons incapable of producing photocurrent.[41] The net result is that one desires a bridge section long enough to minimize charge recombination currents by spatially separating electrons and holes without impeding charge transfer between n-type and p-type sections of the double heterojunction. It is worth pointing out that increases in $V_{OC}$ are commonly observed in energy cascade structures,[42-44] but this fact has yet to be exploited to its full potential for lack of a device structure where voltage and external quantum efficiency (at a given wavelength) can be simultaneously optimized.

Maintaining high cell current requires not only efficient energy transfer, but unimpeded electron transfer between n-type and p-type sections, in turn requiring the appropriate alignment of several key energy levels in the device. The optical gap of the p-type section ($E_P^{OPT}$) is the difference between the HOMO of the p-type section ($E_P^{HOMO}$) and the ionization potential of the singlet exciton ($IP_{S1}$).[45] In general, the energy of the singlet exciton is less than the electronic gap between the LUMO and HOMO levels ($E_P^{LUMO}$ - $E_P^{HOMO}$ ); this difference is the binding energy of the exciton.[46] In the context of the double heterojunction solar cell, the existence of a non-zero exciton binding energy requires an energetic offset between $E_P^{LUMO}$ and the LUMO of the bridge section ($E_B^{LUMO}$) to ensure that electron transfer from the molecular exciton is a thermodynamically favorable process. Naturally, this same consideration applies to hole transfer from the n-type section, requiring the HOMO level of the bridge ($E_B^{HOMO}$) to be equal to or nearer the vacuum level than the electron affinity of the singlet exciton in the n-type section ($EA_{S1}$ see fig. 1). This energetic configuration was calculated to enable solar cell efficiencies approaching 30% even in the presence of a 0.3 eV exciton binding energy.[24]

The combination of electron donating and electron accepting subunits is a very common motif in semiconducting polymers,[10,47-51] and is capable of lowering the optical gap of a material well into the

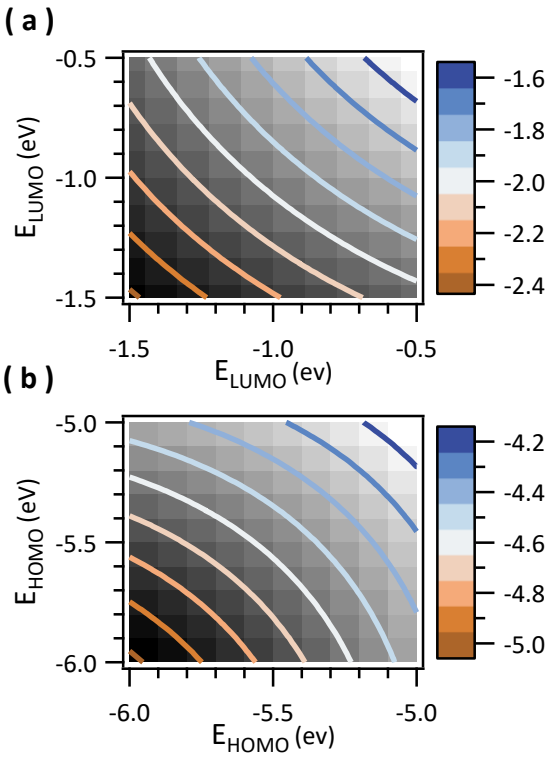


Figure 2. Calculated LUMO (a) and HOMO (b) energies for a series of tetramers as a function of the energies of their subunits.

near infrared, enabling large portions of the solar spectrum to be captured. We constructed a general model of this class of materials by approximating each subunit as a single site with its own HOMO and LUMO levels. The individual sites were allowed to couple to their nearest neighbors and electron-electron repulsion was accounted for in a self-consistent manner according to well established methods.[52] Although this model does not identify synthetic targets without further analysis, it has the advantage of being independent of any particular chemical structure, allowing a wide latitude for the development of specific synthetic targets.

The calculation had three parameters in total, two describing the coupling of nearest-neighbor orbitals (one for the HOMOs and another for the LUMOs), and a third parameter quantifying the strength of electron-electron repulsion. To determine values for these parameters, we calculated the energy of $E^{HOMO}$, $E^{LUMO}$ and $E^{OPT}$ for a series of donor-acceptor tetramers and compared our results to a previous study that employed higher level simulations.[53] The agreement between the calculations is modest, in some instances differing by ±0.5 eV. This lack of precision is due to important structural differences of the molecules in question. Fitting all of them to a single set of parameters without reference to their chemical structures is an approximation. However, the model used here provides us with the opportunity to comment on general, qualitative features of double heterojunction systems.

We used the parameters extracted from the aforementioned calculations to demonstrate the variation of the HOMO and LUMO energies of donor-acceptor tetramers **(D-A)$_4$** as a function of the energy of

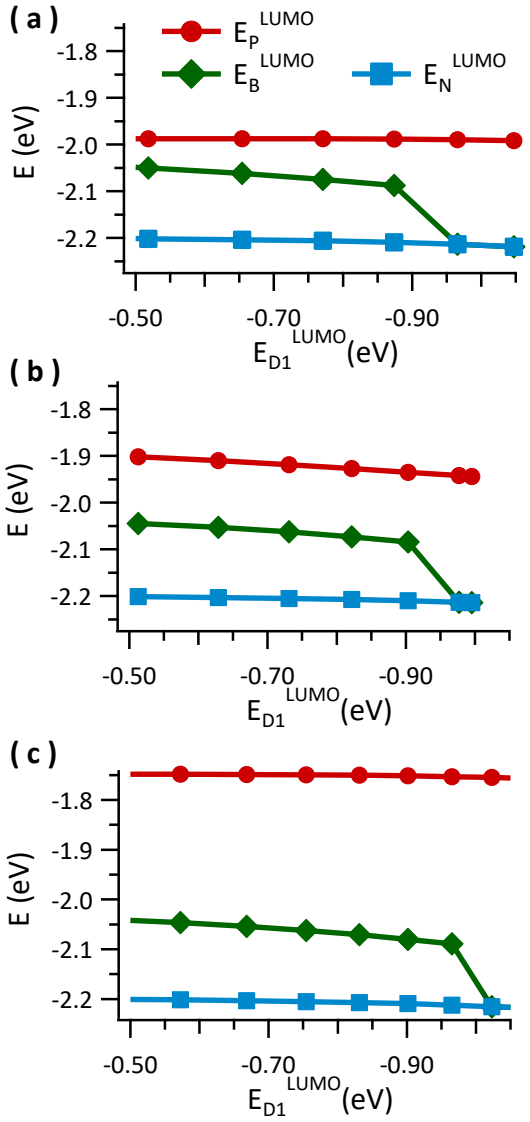


Figure 3. LUMO energies for p-type (red circles) n-type (blue squares) and bridge (green diamonds) sections as a function of one component of the p-type section ($E_{D1}^{LUMO}$). The energy of the complimentary component ($E_{A1}^{LUMO}$) was chosen to keep $E_P^{LUMO}$ of the tetramer unchanged and employed the following energy offsets between p- and n-type sections: (a) 0.2 eV (b) 0.3 eV (c) 0.4 eV.

their subunits. Tetramers are a good approximation of a semi-infinite system as calculations on larger oligomers did not yield significantly different results. The variation of the orbital energies of tetramer systems is shown in Fig. 2. The results are intuitive from the perspective of molecular orbital theory; the strength of the electron-electron repulsion is not strongly dependent on the donor or acceptor energies. As a corollary, our model predicts an exciton binding energy ($E^{EX}$) of 0.31 eV that is independent of tetramer composition.

Using the same parameters as above, we calculated a series of fully conjugated triblock polymers intended as candidates for double heterojunction solar cells. The materials consist of p-type, n-type and bridge sections, the former two again being approximated as tetramers. The p-type section is **(D1-A1)$_4$**, the n-type section is **(D2-A2)$_4$** and the bridge section is a dimer made from the electron donating subunit of the p-type section and the electron accepting subunit of the n-type section (eq. 1).

**(1) (D1-A1)$_4$-(D1-A2)$_2$-(D2-A2)$_4$**

The results of a calculation of the LUMO energies for each section of the polymer is shown in Fig. 3. In performing this calculation, we varied the composition of the bridge while attempting to maintain a constant $E_P^{LUMO}$ using the results of fig. 2. In other words, we varied $E_{D1}^{LUMO}$ and $E_{A1}^{LUMO}$ in such as

way as to follow the contours of Fig 2a for the p-type section while maintaining a fixed $E_{A2}^{LUMO}$. Thus, we varied the bridge composition while attempting to hold the energy levels of the n-type and p-type sections constant relative to the isolated system. We found that maintaining constant energy levels of the p-type and n-type sections was largely possible; the variation was less than 0.1 $eV$. This is the expected behavior if the energies of the p-type and n-type sections are independent of the bridge. In other words, the energy levels of the HOMOs and LUMOs associated with the p-type and n-type sections of a double heterojunction can largely be predicted by examining the polymers individually. However, Fig. 3 demonstrates that the same consideration is not true of the bridge section.

As stated earlier, the components of the bridge are $E_{D1}^{LUMO}$ and $E_{A2}^{LUMO}$ the former of which was varied during the calculations shown in fig 3. There is only a minor variation in the energy of the bridge section until the far right of each graph. At this point, $E_{D1}^{LUMO}$ becomes lower in energy than $E_{A2}^{LUMO}$ and the energy of the bridge drops to become equal to the n-type section. In other words, the energy levels of the bridge are largely independent of its components so long as the electron donating subunits have a smaller electron affinity than the electron accepting subunits. Instead of varying strongly with composition, the energy level of the bridge is pinned to approximately 0.1 - 0.15 eV above the n-type section regardless of the value of $E_P^{LUMO}$.

A similar calculation was performed to determine how the HOMOs are affected by their composition. We fixed the energy of both components in the p-type section and changed the energies of the components in the n-type section, while maintaining a nearly fixed $E_N^{HOMO}$. The results were functionally identical to the ones pictured in Fig. 3. That is, $E_B^{HOMO}$ is pinned below $E_P^{HOMO}$ by a value of 0.15 to 0.1 eV, a nearly optimal energy to allow for unimpeded hole transfer.

As mentioned previously, electron transfer into the bridge from the p-type section should be thermodynamically favorable, while electron transfer into the bridge from the n-type section should be

unfavorable. The first consideration ensures good charge separation, the second inhibits recombination. In symbols, $E_P^{LUMO}$ - $E^{EX} \geq E_B^{LUMO}$ describes the favorability of electron transfer into the bridge, accounting for the binding energy of the molecular exciton, while $E_B^{LUMO} > E_N^{LUMO}$ describes the condition for favorable electron transfer out of the bridge. Maximum device efficiency is predicted to occur when $E_P^{LUMO}$ - $E^{EX} = E_B^{LUMO}$ and $E_B^{LUMO} = E_N^{LUMO}$+0.05 eV.[24] The calculations of Fig. 3 show that for our double heterojunction materials, $E_B^{LUMO} \approx E_N^{LUMO}$+0.1 eV while $E_P^{LUMO}$ can be tuned independently of $E_B^{LUMO}$. Thus, it should be possible to satisfy the requirements for a functioning double heterojunction cell by choosing n-type and p-type materials with offsets 0.1 eV greater than the exciton binding energy, and forming the bridge according to eq. 1. Although the energetic position of the bridge appears to be pinned above the n-type section to an amount slightly greater than is optimal in terms of device efficiency, the additional amount of offset is an advantage from the perspective of an initial synthetic approach.

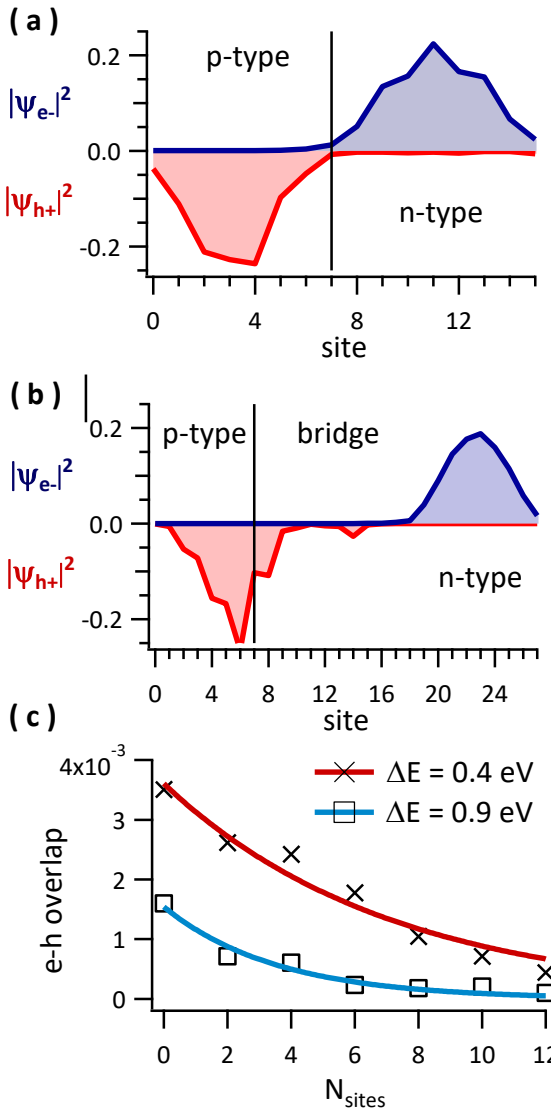


Figure 4. Lowest energy excited states. (a) offset of 0.4 eV without a bridge section. (b) offset of 0.9 eV with bridge of 6 monomer units (12 sites). Red illustrates hole density and blue illustrates electron density. (c) spatial overlap between electron and hole density for a series of double heterojunction systems.

Another important design parameter to specify in a double heterojunction material is the length of the bridge section. In order to estimate the magnitude of recombination currents as a function of bridge length, a series of double heterojunction materials were

calculated. The materials had n-type and p-type sections with identical optical gaps and differed in terms of the length of the bridge section ($N = 2N_{sites}$) and the energetic offset (ΔE) between the n-type and p-type orbitals.

**(2) $(D1\text{-}A1)_4\text{-}(D1\text{-}A2)_N\text{-}(D2\text{-}A2)_4$**

The excited states were calculated self-consistently to find the charge separated state in a manner very similar to the calculation of the ground states of the system. Fig 4a shows the lowest energy excited state of a diblock polymer (i.e. having no bridge) and an energetic offset between ΔE=0.4 eV. Fig. 4b shows a triblock system with a bridge length of 6 repeat units (12 sites total) and an energy offset of ΔE=0.9 eV. Because of the strong electronic coupling between sites, the spatial overlap between electron and hole wavefunctions is larger in Fig. 4a. This implies that the recombination rate should be significantly higher in the absence of a bridge section as significant electron density leaks into the p-type section and significant hole density leaks into the n-type section. An estimate of the recombination rate for a series of double heterojunction materials can be made by multiplying the electron and the hole probability densities on each site and summing over all sites. Fig. 4c shows the result for two different energy offsets between the p-type and n-type sections. As the length of the bridge increases, the electron/hole overlap decreases; this decrease is more pronounced for larger energy offsets. Our previous report indicated that approximately 5 nm of bridge length was sufficient to eliminate the effect of tunneling currents through the bridge. A similar length also seems effective at lowering the overlap of electron and hole wavefunctions by an order of magnitude relative to the corresponding diblock system.

The length of the p-type and n-type sections also plays an important role in the proposed double heterojunction structure. As stated briefly above, optimum efficiency occurs only when all recombination currents occur through the bridge. This requires a complete absence of direct connections between p-type and n-type sections, in other words, completely pure phases of the block polymer.[24]

Although the phase behavior of rigid-rod block polymers[54] is not explored to the extent of coil and rod-coil block polymers[55-57] phase separation is thermodynamically favored in the case of infinitely long random-coil chains.[58,59] Thus, higher solar cell efficiencies are likely to be obtained for longer p-type and n-type sections. In addition, work by the McGehee group indicates that a complex hierarchical morphology is an important aspect of a high performance bulk heterojunction.[60] Because the optimal morphology of a double heterojunction system is likely the thermodynamically favorable state, it has an important advantage relative to the bulk heterojunction, especially in terms of large scale production.

A series of self-consistent field calculations on a generalized donor-acceptor structure for block polymer based organic double heterojunction materials was performed. The structure contains a p-type section and an n-type section connected via a bridge section that is composed of one subunit from each. The results show that the energy of the n-type and p-type sections are largely independent of one another. Moreover the LUMO (HOMO) of the bridge section does not strongly depend upon its constituents, but is pinned to just above the LUMO of the n-type (just below the HOMO of the p-type) section. Thus, proper energy alignment for the system can be achieved by choosing p-type and n-type materials with an energy offset slightly greater than the exciton binding energy, forming the bridge from their components according to fig. 1. The length of the bridge has an important effect on the overlap between electron and hole wavefunctions in the charge separated state. This overlap is minimized for long bridge sections with large energy offsets between n-type and p-type sections. In addition, the length of the p-type and n-type sections should be made as large as possible to achieve the necessary degree of phase separation.

## COMPUTATIONAL METHODS

Conjugated polymers made from electron donating and electron accepting subunits were modeled by approximating each subunit as a single site with two energy levels, the HOMO and the LUMO. The self-

consistent field calculations were performed according to well-established prescriptions.[52] Each site was allowed to couple to its nearest neighbors, the strength of the coupling between adjacent HOMOs was parameterized independently from the strength of the coupling between adjacent LUMOs. Solving the resulting eigenvector problem produces a set of solutions in the absence of electron-electron repulsion. These were used as a basis set for the self-consistent field calculations. Repulsion between the eigenvectors was calculated by representing each eigenvector in the site basis and taking the product of their probability densities on each site $|c_i|^2$. The total repulsion is the sum of these products multiplied by a parameter $\gamma$ used to quantify the strength of this repulsive interaction. In symbols, the total repulsion between eigenvectors 1 and 2 is given by the following:

(3) $\Gamma_{12} = \sum_i^N \gamma |c_{i1}|^2 |c_{i2}|^2$

The eigenvector problem in the presence of electron-electron repulsion was solved iteratively until the orbital energies converged, typically requiring less than 10 iterations.

The excited states of the system were also calculated self-consistently. The initial guesses were generated by removing an electron from an occupied ground state orbital and placing it into an unoccupied orbital to create a basis set of multiparticle wavefunctions. The self-consistent multiparticle wavefunctions were calculated by considering the electron-electron repulsion between them in a manner similar to the ground state calculation.

In order to make an unambiguous connection to previously published estimates of solar cell efficiency,[24] it was necessary to assign states to the p-type, bridge, and n-type sections of the double heterojunction. Although such distinctions are somewhat artificial, we employed an algorithm that gave a wide latitude to the necessary parameters with the intent of sorting states as objectively as possible. The algorithm for sorting the ground state wavefunctions produced results insensitive to small variations in the sorting parameters; it proceeds in several steps. First, the system was divided into three sections,

defining a demarcation between p-type, bridge and n-type sections. This definition essentially determines the length of the bridge and was not fixed, but allowed to vary in search of the optimal solution. The demarcation was allowed to vary symmetrically from the bridge position as defined in eq. 1 to plus or minus two sites. Second, the total probability density for each section was found by summing the probability density of each state over the appropriate sites. A state was then assigned to a section if its total probability density for that section was greater than a threshold value. The threshold value was also allowed to vary to find the optimal solution. However, before finding the optimal value for the two sorting parameters, we rejected any solution that did not meet two requirements. In a valid solution, every state is assigned to at least one section and every section is assigned at least one state. However, we did not require that a state be assigned to only one section, because there were many states that were equally shared among multiple sections.

The result of these considerations was a set of solutions that differed by the value of the two sorting parameters. Clearly, a state does not belong to a section if the total probability density for that section is near zero, far from the threshold. Conversely, an assignment is strong if the total probability density for that section exceeds the threshold by a large margin. Thus, a margin of exclusion or inclusion could be defined by the absolute value of the difference between the probability density and threshold. An ideal assignment has both large margins of inclusion and exclusion. Maximizing the product of these margins produces the optimal values of the sorting parameters. The optimal threshold value was typically near the largest values which still produced valid assignments. The optimal bridge length typically corresponded to the definition found in eq. 1. As stated above, minor variations in the values of the sorting parameters did not change the assignments.

AUTHOR INFORMATION

lkaake@sfu.ca

**Notes**

The author declares no competing financial interest.

ACKNOWLEDGMENT

L.G.K. acknowledges the support of the Natural Science and Engineering Research Council (NSERC) of Canada under the Discovery Grant Program.

REFERENCES

(1) Green, M. A. Commercial Progress and Challenges for Photovoltaics. *Nat. Energy* **2016**, *1*, 15015.

(2) Haegel, N. M.; Margolis, R.; Buonassisi, T.; Feldman, D.; Froitzheim, A.; Garabedian, R.; Green, M.; Glunz, S.; Henning, H.-M.; Holder, B.et al. Terawatt-Scale Photovoltaics: Trajectories and Challenges. *Science* **2017**, *356*, 141-143.

(3) Tang, C. W. 2-Layer Organic Photovoltaic Cell. *Appl. Phys. Lett.* **1986**, *48*, 183-185.

(4) Yu, G.; Gao, J.; Hummelen, J. C.; Wudl, F.; Heeger, A. J. Polymer Photovoltaic Cells - Enhanced Efficiencies Via a Network of Internal Donor-Acceptor Heterojunctions. *Science* **1995**, *270*, 1789-1791.

(5) Halls, J. J. M.; Pichler, K.; Friend, R. H.; Moratti, S. C.; Holmes, A. B. Exciton Diffusion and Dissociation in a Poly(p-phenylenevinylene)/C-60 Heterojunction Photovoltaic Cell. *Appl. Phys. Lett.* **1996**, *68*, 3120-3122.

(6) Sun, J.; Jasieniak, J. J. Semi-Transparent Solar Cells. *J. Phys. D. Appl. Phys.* **2017**, *50*, 093001.

(7) He, Z. C.; Xiao, B.; Liu, F.; Wu, H. B.; Yang, Y. L.; Xiao, S.; Wang, C.; Russell, T. P.; Cao, Y. Single-Junction Polymer Solar Cells with High Efficiency and Photovoltage. *Nat. Photonics* **2015**, *9*, 174-179.

(8) Zhao, W.; Qian, D.; Zhang, S.; Li, S.; Inganäs, O.; Gao, F.; Hou, J. Fullerene-Free Polymer Solar Cells with Over 11% Efficiency and Excellent Thermal Stability. *Adv. Mater.* **2016**, *28*, 4734-4739.

(9) Li, S.; Ye, L.; Zhao, W.; Zhang, S.; Mukherjee, S.; Ade, H.; Hou, J. Energy-Level Modulation of Small-Molecule Electron Acceptors to Achieve over 12% Efficiency in Polymer Solar Cells. *Adv. Mater.* **2016**, 9423-9429.

(10) Scharber, M. C.; Wuhlbacher, D.; Koppe, M.; Denk, P.; Waldauf, C.; Heeger, A. J.; Brabec, C. L. Design Rules for Donors in Bulk-heterojunction Solar Cells - Towards 10 % Energy-Conversion Efficiency. *Adv. Mater.* **2006**, *18*, 789-794.

(11) Lee, M. M.; Teuscher, J.; Miyasaka, T.; Murakami, T. N.; Snaith, H. J. Efficient Hybrid Solar Cells Based on Meso-Superstructured Organometal Halide Perovskites. *Science* **2012**, *338*, 643-647.

(12) Tan, H. R.; Jain, A.; Voznyy, O.; Lan, X. Z.; de Arquer, F. P. G.; Fan, J. Z.; Quintero-Bermudez, R.; Yuan, M. J.; Zhang, B.; Zhao, Y. C.et al. Efficient and Stable Solution-Processed Planar Perovskite Solar Cells via Contact Passivation. *Science* **2017**, *355*, 722-726.

(13) Scharber, M. C. On the Efficiency Limit of Conjugated Polymer:Fullerene-Based Bulk Heterojunction Solar Cells. *Adv. Mater.* **2016**, *28*, 1994-2001.

(14) Janssen, R. A. J.; Nelson, J. Factors Limiting Device Efficiency in Organic Photovoltaics. *Adv. Mater.* **2013**, *25*, 1847-1858.

(15) Hong, Z. R.; Lessmann, R.; Maennig, B.; Huang, Q.; Harada, K.; Riede, M.; Leo, K. Antenna Effects and Improved Efficiency in Multiple Heterojunction Photovoltaic Cells Based on Pentacene, Zinc Phthalocyanine, and C60. *J. Appl. Phys.* **2009**, *106*, 064511.

(16) Heidel, T. D.; Hochbaum, D.; Sussman, J. M.; Singh, V.; Bahlke, M. E.; Hiromi, I.; Lee, J.; Baldo, M. A. Reducing Recombination Losses in Planar Organic Photovoltaic Cells Using Multiple Step Charge Separation. *J. Appl. Phys.* **2011**, *109*, 104502.

(17) Barito, A.; Sykes, M. E.; Huang, B. Y.; Bilby, D.; Frieberg, B.; Kim, J.; Green, P. F.; Shtein, M. Universal Design Principles for Cascade Heterojunction Solar Cells with High Fill Factors and Internal Quantum Efficiencies Approaching 100%. *Adv. Energy Mater.* **2014**, *4*, 1400216.

(18) Cnops, K.; Rand, B. P.; Cheyns, D.; Verreet, B.; Empl, M. A.; Heremans, P. 8.4% Efficient Fullerene-Free Organic Solar Cells Exploiting Long-Range Exciton Energy Transfer. *Nat. Commun.* **2014**, *5*, 3406.

(19) Menke, S. M.; Holmes, R. J. Energy-Cascade Organic Photovoltaic Devices Incorporating a Host–Guest Architecture. *ACS Appl. Mater. Interfaces* **2015**, *7*, 2912-2918.

(20) Cheng, P.; Zhan, X. Versatile Third Components for Efficient and Stable Organic Solar Cells. *Mater. Horiz.* **2015**, *2*, 462-485.

(21) Lessard, B. H.; Dang, J. D.; Grant, T. M.; Gao, D.; Seferos, D. S.; Bender, T. P. Bis(tri-n-hexylsilyl oxide) Silicon Phthalocyanine: A Unique Additive in Ternary Bulk Heterojunction Organic Photovoltaic Devices. *ACS Appl. Mater. Interfaces* **2014**, *6*, 15040-15051.

(22) Busby, E.; Xia, J.; Wu, Q.; Low, J. Z.; Song, R.; Miller, J. R.; Zhu, X. Y.; Campos, Luis M.; Sfeir, M. Y. A Design Strategy for Intramolecular Singlet Fission Mediated by Charge-Transfer States in Donor–Acceptor Organic Materials. *Nat. Mater.* **2015**, *14*, 426-433.

(23) Reusswig, P. D.; Congreve, D. N.; Thompson, N. J.; Baldo, M. A. Enhanced External Quantum Efficiency in an Organic Photovoltaic Cell via Singlet Fission Exciton Sensitizer. *Appl. Phys. Lett.* **2012**, *101*, 113304.

(24) Hutnan, M. P. J.; Kaake, L. G. Design Principles for Block Polymer Organic Double Heterojunction Solar Cells. *Mater. Horiz.* **2016**, *3*, 575-580.

(25) Hadziioannou, G. Semiconducting Block Copolymers for Self-Assembled Photovoltaic Devices. *MRS Bull.* **2002**, *27*, 456-460.

(26) Sivula, K.; Ball, Z. T.; Watanabe, N.; Frechet, J. M. J. Amphiphilic Diblock Copolymer Compatibilizers and their Effect on the Morphology and Performance of Polythiophene: Fullerene Solar Cells. *Adv. Mater.* **2006**, *18*, 206-210.

(27) Sun, S. S.; Zhang, C.; Ledbetter, A.; Choi, S.; Seo, K.; Bonner, C. E.; Drees, M.; Sariciftci, N. S. Photovoltaic Enhancement of Organic Solar Cells by a Bridged Donor-Acceptor Block Copolymer Approach. *Appl. Phys. Lett.* **2007**, *90*, 043117.

(28) Zhang, Q. L.; Cirpan, A.; Russell, T. P.; Emrick, T. Donor-Acceptor Poly(thiophene-block-perylene diimide) Copolymers: Synthesis and Solar Cell Fabrication. *Macromolecules* **2009**, *42*, 1079-1082.

(29) Tao, Y. F.; McCulloch, B.; Kim, S.; Segalman, R. A. The Relationship Between Morphology and Performance of Donor-Acceptor Rod-Coil Block Copolymer Solar Cells. *Soft Matter* **2009**, *5*, 4219-4230.

(30) Sary, N.; Richard, F.; Brochon, C.; Leclerc, N.; Leveque, P.; Audinot, J. N.; Berson, S.; Heiser, T.; Hadziioannou, G.; Mezzenga, R. A New Supramolecular Route for Using Rod-Coil Block Copolymers in Photovoltaic Applications. *Adv. Mater.* **2010**, *22*, 763-768.

(31) Sommer, M.; Huettner, S.; Thelakkat, M. Donor-Acceptor Block Copolymers for Photovoltaic Applications. *J. Mater. Chem.* **2010**, *20*, 10788-10797.

(32) Ren, G. Q.; Wu, P. T.; Jenekhe, S. A. Solar Cells Based on Block Copolymer Semiconductor Nanowires: Effects of Nanowire Aspect Ratio. *ACS Nano* **2011**, *5*, 376-384.

(33) Botiz, I.; Schaller, R. D.; Verduzco, R.; Darling, S. B. Optoelectronic Properties and Charge Transfer in Donor-Acceptor All-Conjugated Diblock Copolymers. *J. Phys. Chem. C* **2011**, *115*, 9260-9266.

(34) Ku, S. Y.; Brady, M. A.; Treat, N. D.; Cochran, J. E.; Robb, M. J.; Kramer, E. J.; Chabinyc, M. L.; Hawker, C. J. A Modular Strategy for Fully Conjugated Donor-Acceptor Block Copolymers. *J. Am. Chem. Soc.* **2012**, *134*, 16040-16046.

(35) Guo, C.; Lin, Y.-H.; Witman, M. D.; Smith, K. A.; Wang, C.; Hexemer, A.; Strzalka, J.; Gomez, E. D.; Verduzco, R. Conjugated Block Copolymer Photovoltaics with Near 3% Efficiency Through Microphase Separation. *Nano Lett.* **2013**, *13*, 2957-2963.

(36) Kozycz, L. M.; Gao, D.; Hollinger, J.; Seferos, D. S. Donor–Donor Block Copolymers for Ternary Organic Solar Cells. *Macromolecules* **2012**, *45*, 5823-5832.

(37) Wang, J.; Higashihara, T. Synthesis of All-Conjugated Donor Acceptor Block Copolymers and their Application in All-Polymer Solar Cells. *Polym. Chem.* **2013**, *4*, 5518-5526.

(38) Wang, J.; Ueda, M.; Higashihara, T. Synthesis and Morphology of All-Conjugated Donor- Acceptor Block Copolymers Based on Poly( 3-hexylthiophene) and Poly( naphthalene diimide). *J. Polym. Sci. Pol. Chem.* **2014**, *52*, 1139-1148.

(39) Lin, Y. H.; Yager, K. G.; Stewart, B.; Verduzco, R. Lamellar and Liquid Crystal Ordering in Solvent-Annealed All-Conjugated Block Copolymers. *Soft Matter* **2014**, *10*, 3817-3825.

(40) Lee, Y. H.; Chen, W. C.; Chiang, C. J.; Kau, K. C.; Liou, W. S.; Lee, Y. P.; Wang, L.; Dai, C. A. A New Strategy for Fabricating Organic Photovoltaic Devices with Stable D/A Double-Channel Network to Enhance Performance Using Self-Assembling All-Conjugated Diblock Copolymer. *Nano Energy* **2015**, *13*, 103-116.

(41) Rao, A.; Chow, P. C. Y.; Gelinas, S.; Schlenker, C. W.; Li, C.-Z.; Yip, H.-L.; Jen, A. K. Y.; Ginger, D. S.; Friend, R. H. The Role of Spin in the Kinetic Control of Recombination in Organic Photovoltaics. *Nature* **2013**, *500*, 435-439.

(42) Sista, S.; Yao, Y.; Yang, Y.; Tang, M. L.; Bao, Z. Enhancement in Open Circuit Voltage Through a Cascade-Type Energy Band Structure. *Appl. Phys. Lett.* **2007**, *91*, 223508.

(43) Khlyabich, P. P.; Burkhart, B.; Thompson, B. C. Compositional Dependence of the Open-Circuit Voltage in Ternary Blend Bulk Heterojunction Solar Cells Based on Two Donor Polymers. *J. Am. Chem. Soc.* **2012**, *134*, 9074-9077.

(44) Nakano, K.; Suzuki, K.; Chen, Y. J.; Tajima, K. Roles of Energy/Charge Cascades and Intermixed Layers at Donor/Acceptor Interfaces in Organic Solar Cells. *Sci. Rep.* **2016**, *6*, 29529.

(45) Zhu, X. Y. How to Draw Energy Level Diagrams in Excitonic Solar Cells. *J. Phys. Chem. Lett.* **2014**, *5*, 2283-2288.

(46) Bredas, J.-L. Mind the Gap! *Mater. Horiz.* **2014**, *1*, 17-19.

(47) Brabec, C. J.; Winder, C.; Sariciftci, N. S.; Hummelen, J. C.; Dhanabalan, A.; van Hal, P. A.; Janssen, R. A. J. A Low-Bandgap Semiconducting Polymer for Photovoltaic Devices and Infrared Emitting Diodes. *Adv. Funct. Mater.* **2002**, *12*, 709-712.

(48) Winder, C.; Sariciftci, N. S. Low Bandgap Polymers for Photon Harvesting in Bulk Heterojunction Solar Cells. *J. Mater. Chem.* **2004**, *14*, 1077-1086.

(49) Park, S. H.; Roy, A.; Beaupre, S.; Cho, S.; Coates, N.; Moon, J. S.; Moses, D.; Leclerc, M.; Lee, K.; Heeger, A. J. Bulk Heterojunction Solar Cells with Internal Quantum Efficiency Approaching 100%. *Nat. Photonics* **2009**, *3*, 297-302.

(50) Liang, Y. Y.; Yu, L. P. A New Class of Semiconducting Polymers for Bulk Heterojunction Solar Cells with Exceptionally High Performance. *Accounts Chem. Res.* **2010**, *43*, 1227-1236.

(51) Yao, H.; Ye, L.; Zhang, H.; Li, S.; Zhang, S.; Hou, J. Molecular Design of Benzodithiophene-Based Organic Photovoltaic Materials. **2016**, *116*, 7397-7457.

(52) Szabo, A.; Ostlund, N. S. *Modern Quantum Chemistry: Introduction to Advanced Electronic Structure Theory*; Dover Publications, 1989.

(53) Pandey, L.; Risko, C.; Norton, J. E.; Bredas, J. L. Donor-Acceptor Copolymers of Relevance for Organic Photovoltaics: A Theoretical Investigation of the Impact of Chemical Structure Modifications on the Electronic and Optical Properties. *Macromolecules* **2012**, *45*, 6405-6414.

(54) Segalman, R. A.; McCulloch, B.; Kirmayer, S.; Urban, J. J. Block Copolymers for Organic Optoelectronics. *Macromolecules* **2009**, *42*, 9205-9216.

(55) Bates, F. S.; Fredrickson, G. H. Block Copolymers - Designer Soft Materials. *Phys. Today* **1999**, *52*, 32-38.

(56) Park, C.; Yoon, J.; Thomas, E. L. Enabling Nanotechnology with Self Assembled Block Copolymer Patterns. *Polymer* **2003**, *44*, 6725-6760.

(57) Darling, S. B. Block Copolymers for Photovoltaics. *Energy Environ. Sci.* **2009**, *2*, 1266-1273.

(58) Flory, P. J. *Principles of Polymer Chemistry*; Cornell University Press: Ithica, NY; 1953.

(59) Hiemenz, P. C.; Lodge, T. P. *Polymer Chemistry, Second Edition*; CRC Press: Boca Raton, FL; 2007.

(60) Burke, T. M.; McGehee, M. D. How High Local Charge Carrier Mobility and an Energy Cascade in a Three-Phase Bulk Heterojunction Enable > 90% Quantum Efficiency. *Adv. Mater.* **2014**, *26*, 1923-1928.